A New Compact Finline OMT Based on Multi-Section Transformer

Yaqing Yu, Wen Jiang, Shuai Zhang, Shuxi Gong, and Tong Cheng

National Key Laboratory of Antennas and Microwave Technology
Xidian University, Xi'an, 710071, China
yuyaqing27@163.com, jw13@vip.qq.com, zhangshuai@xidian.edu.cn, shxgong@xidian.edu.cn,
chengtong26@163.com

Abstract ─ In the millimeter wave band, the simplification of the orthomode transducer (OMT)'s structure and processing technic is placed in a more important position. The finline OMT can meet the requirement, but its size is usually not compact enough. To solve this problem, a compact finline OMT based on multi-section transformer is presented. Such OMT can enable size reduction by reasonably designing three transformers to reach the matching condition, which makes the design more flexible. As a result, the -20dB reflection bandwidth of the proposed OMT is 30.2 GHz to 49.8 GHz (49%), while the lengths of main arm's and side arm's transition for vertical polarization are $1.35\lambda_{max}$ and $0.9\lambda_{max}$ (λ_{max} denotes the maximum free space wavelength in band), respectively, which has been greatly reduced compared with the traditional ones. To verify the working performance of the design, a prototype is fabricated and measured. Finally, some assembly errors are analyzed to study its influence. The results show that the proposed OMT can be a good candidate for millimeter wave application.

Index Terms ─ Compact, finline OMT, millimeter wave application, multi-section transformer.

I. INTRODUCTION

An orthomode transducer (OMT) can separate or combine two orthogonal polarizations to double the channel capacity. In recent years, with the development of remote sensing and radio astronomy, the demands for the high operating frequency and the ultra-wideband characteristics of the receiver system are on the rise. At millimeter wave band, the physical size of the device becomes smaller, thus leading to the higher demands for machining and assembly process. To fulfill these requirements, it is necessary to expand the bandwidth of the OMT and reduce its complexity.

Generally, OMTs can be divided into planar type and waveguide type. The planar OMTs are mainly based on microstrip line structure, which have the shortcomings of large insertion loss, low power capacity and poor matching with the waveguide [1,2].

Waveguide OMTs have many merits, such as high power capacity and mechanical robustness. To achieve wideband applications, it is necessary to suppress the higher order modes, such as TE_{11} and TM_{11} modes in a square waveguide [3]. For asymmetric OMT, their fractional working bandwidth can only reach about 20%, for the higher order modes cannot be controlled effectively [4,5].

As the suppression of higher order modes is found related to the symmetry of the OMT's topology, the two-fold symmetric structure has the best effect, which separates both polarizations' power into two halves, and then can be recombined later. The representative forms are Turnstile OMT [6-9] and Bøifot OMT [9-11], featuring the advantages of broadband, high isolation, high cross-polarization discrimination, and low insertion loss. However, they all have complicated structures and usually need to be divided into three or more blocks for processing, which will introduce a lot of assembly errors in millimeter frequency range.

One-fold symmetric structure means only one of the polarizations' power will be separated and recombined, which can suppress the odd higher order modes. In general, the finline one [12-16] and the transformations of the Bøifot OMT that are based on the double ridge transition [17-20] and the reverse coupling structure [21] can be concluded as the one-folded symmetric type. The former can achieve a bandwidth of 40%-60% and will be discussed later. The latter require a height-reduced waveguide to make the higher order modes evanescent, but the transition from the double ridge to the output port will limit the OMT performance for its vertical polarization. In general, their reported working bandwidth are no more than 50%. In addition, their structures are also complicated and bulky.

In other OMTs, the quad-ridged one [22,23] also needs the absorber, and its transition needs to match the hundreds of ohms waveguide with the 50 ohms coaxial cables. Therefore, it usually needs a long transition to ensure the in-band reflection characteristic. The OMT based on the SIW [24] and the polarization-selective coupling structure [25] belong to the asymmetric type,

Submitted On: May 18, 2018
Accepted On: October 19, 2018

which both have the disadvantage of narrow bandwidth.

The proposed OMT chooses the finline form, which was first presented by Roberson [12] with the characteristics of ultra-wideband operation and simple structure. It can be manufactured with two blocks and a metal plate, so the advantage of easy fabrication makes it a good candidate for millimeter wave or terahertz application [13]. For this OMT, the main drawback is its large size, and the traditional linear or exponential double ridge transitions usually require a long transition to guarantee the matching characteristics for vertical polarization. For instance, the linear transition is used in [14] and [15], and one of them can achieve a -20dB impedance fractional bandwidth of about 52%, when its main arm's and the side arm's double ridge transition lengths are $3.2\lambda_{max}$ and $1.8\lambda_{max}$ (λ_{max} denotes the maximum free space wavelength in band), respectively. For the exponential case [13], it realizes a -15dB impedance bandwidth of 42% in the terahertz band, while the transitions' lengths are both reduced to $1.4\lambda_{max}$. In addition, the transitions' lengths have been further reduced to $0.54\lambda_{max}$ and $0.48\lambda_{max}$ to enhance the isolation performance with the expense of narrow bandwidth [16]. Therefore, ensuring both miniaturization and high performance is still a problem for finline OMT.

In this paper, a finline OMT based on multi-section transformer is developed to solve the problem above. It works at 7mm-band (30GHz-50GHz), which is used for the detection of interstellar molecular line in radio astronomy. The multi-section transformer is widely used in waveguide matching [6], slot antenna profile reduction [26] and power divider impedance transformation [27]. However, to the best of our knowledge, the multi-section transformer has never been used to achieve the miniaturization of the finline OMT. The comparison between other OMTs and the proposed one is listed in Table 1.

The rest of the paper is arranged as follows. Section II mainly describes the theory of the multi-section transformer. The design of the multi-section transformers and OMT is put in Section III. In Section IV, a prototype is fabricated and tested to verify the proposed structure, and some error analyses are carried out. Finally, a brief summary is shown in Section V.

Table 1: The comparison between the other OMTs and the proposed one

Ref.	OMT Type	S11/dB	Bandwidth	Isolation /dB	Insertion loss /dB	Cross Pol. /dB	Size/λ_{max}^3	Complexity
[2]	Planar	<-15	41.2%		<-2	<-58		Simple
[5]	Asym.	<-22.5	12.1%	>65		<-57	1.7×2.3×0.86 (model size)	Simple
[6]	Turnstile	<-25	37%	>50	<0.2	<-50	3.4×5.2×6.8 (fabricated size)	Complex
[9]	Turnstile Bøifot	<-24 <-29	57.5% 36.6%	>40	<0.11		0.94×1.56×1.73 1.17×1.35×1.53 (model size)	Complex
[10]	Bøifot	<-28	40%	>47	<0.5	<-40		Complex
[17]	Double ridged	<-20	49.7%	>45	<0.16		4.74×4.74×5.69 (fabricated size)	Medium
[20]	Double ridged	<-20	40%	>60			2.15×1.05×4.43 (model size)	Medium
[21]	Reverse Coupling	<-20	32%	>50	<0.2	<-30		Medium
[22]	Quad-ridged	<-15	72%	>50	<3	<-55	0.8 (transition length)	Simple
[13]	Exp. finline	<-15	42%	>55	<1.7	<-57	1.4, 1.4 (transition length)	Simple
[15]	Linear finline	<-20	52%	>40		<-20	3.2, 1.8 (transition length)	Simple
This work	Stepped finline	<-20	49%	>67	<1.1	<-76	1.35, 0.9 (transition length) 2.86×3.43×4.12 (fabricated size) 0.97×3.27×2.18 (model size)	Simple

II. THEORY OF THE MULTI-SECTION TRANSFORMER

To facilitate a brief analysis of the working characteristics of the transformer, a simple model is given here. The transformer achieves the impedance matching from Z_0 to Z_L, and its fundamental circuit diagram is shown in Fig. 1. To simplify the analysis, we only discuss the case that the electrical lengths of all sections are equal [28]. The normalized complex matrix $\bar{A}$ of the transformation from Z_0 to Z_L can be written as:

$$\bar{A}=\begin{bmatrix}\bar{a} & \bar{b}\\ \bar{c} & \bar{d}\end{bmatrix}=\begin{bmatrix}\sqrt{\frac{Z_1}{Z_0}} & 0\\ 0 & \sqrt{\frac{Z_0}{Z_1}}\end{bmatrix}\begin{bmatrix}\cos\theta & j\sin\theta\\ -j\sin\theta & \cos\theta\end{bmatrix}\cdots$$
$$\begin{bmatrix}\sqrt{\frac{Z_N}{Z_{N-1}}} & 0\\ 0 & \sqrt{\frac{Z_{N-1}}{Z_N}}\end{bmatrix}\begin{bmatrix}\cos\theta & j\sin\theta\\ -j\sin\theta & \cos\theta\end{bmatrix}\begin{bmatrix}\sqrt{\frac{Z_L}{Z_N}} & 0\\ 0 & \sqrt{\frac{Z_N}{Z_L}}\end{bmatrix}, \quad (1)$$

where Z_1, …Z_{N-1}, Z_N, are the characteristic impedance of each section of the transformer, Z_L and Z_0 are the Port 1 and Port 2's input resistance, respectively. $\theta=\beta l$, and $\bar{a}$, $\bar{b}$, $\bar{c}$, $\bar{d}$ are the elements of the normalized complex matrix $\bar{A}$.

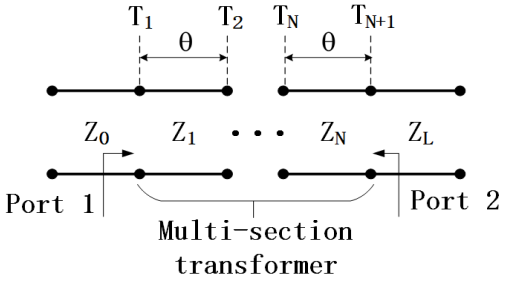

Fig. 1. Fundamental circuit diagram of multi-section impedance transformer.

Then, we can use $\bar{a}$, $\bar{b}$, $\bar{c}$, and $\bar{d}$ in (1) to express the attenuation L:

$$L=\frac{1}{|S_{21}|^2}=\frac{1}{4}\left|\bar{a}+\bar{b}+\bar{c}+\bar{d}\right|^2 . \quad (2)$$

As is known, the moduli of two complex numbers with mutual conjugation are equal:

$$\frac{1}{4}\left|\bar{a}+\bar{b}+\bar{c}+\bar{d}\right|^2=\frac{1}{4}\left|\bar{a}^*+\bar{b}^*+\bar{c}^*+\bar{d}^*\right|^2 , \quad (3)$$

where $\bar{a}^*$, $\bar{b}^*$, $\bar{c}^*$, $\bar{d}^*$ are the elements of the complex conjugate matrix $\bar{A}^*$.

Because j and $\sin\theta$ always appear at the same time in (1), the elements of the complex conjugate matrix $\bar{A}^*$ can be regarded as turning all $\sin\theta$ to $-\sin\theta$. According to (3), it is not difficult for us to figure out that the expression of L only contains the even power of $\sin\theta$. Because $\sin^2\theta=1-\cos^2\theta$, the formula of L can be expressed as the even power of $\cos\theta$:

$$L=\sum_{i=0}^{N}A_i\cos^{2i}\theta , \quad (4)$$

where $A_i=A_i(Z_1,\ldots Z_{N-1},Z_N,Z_L),(i=0,1,2,\ldots N)$.

Since the matching condition of input port 1 is L=1, (4) can be rewritten as:

$$\sum_{i=0}^{N}A_i\cos^{2i}\theta-1=0 . \quad (5)$$

When all the coefficients satisfy certain conditions (by adjusting Z_0, Z_1, … Z_{N-1}, Z_N, Z_L), (5) can get N real roots, which is equivalent to the N zeros of its frequency response curve. By properly selecting the impedance values of each section of the transformer, it can always make full match at these frequency points, so as to realize a well-matched characteristic over a specified band. For the case that the electrical lengths of these sections are different, the corresponding proof process is given by [29].

Based on the ideas above, three transformers are designed in Section III.

III. OMT CONFIGURATION

The proposed OMT is shown in Fig. 2, including a T-type waveguide, a slotted metal plate and an absorber. The T-type waveguide is composed of a main arm and a side arm, in which three transformers are contained.

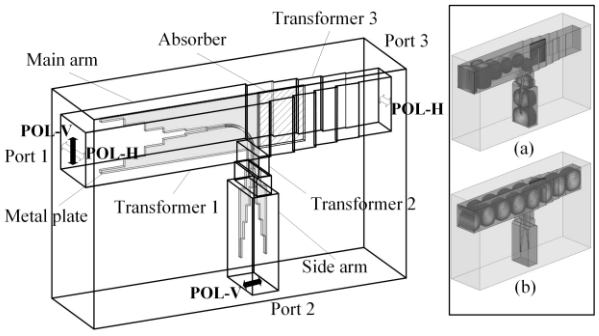

Fig. 2. General configuration of stepped double ridge structure based finline OMT. The inset describes the field distributions of the OMT at 37.5 GHz under vertical (a) and horizontal (b) polarizations.

When the vertical polarization is stimulated at the OMT's common Port 1, the field distribution is shown in the inset (a) of Fig. 2. The energy of TE_{10} mode is gradually transformed and confined to the finline gap via the main arm's transition (Transformer 1). Then the energy will be guided into the side arm by a 90-degree bend and be transferred to the port 2 by the side arm's transition (Transformer 2). When the vertical polarization is excited, the energy of TE_{01} mode travels through the metal plate virtually unperturbed by undergoing the

process of separation and recombination [14]. After passing through the transformer 3, the energy will be eventually output by Port 3, which is depicted in the inset (b) of Fig. 2. In addition, to suppress the excitation of unwanted modes generated by the double ridge, an absorber is inserted [14].

It can be concluded that the OMT's matching characteristic is determined by the three transformers and the 90-degree bend. As the 90-degree bend is easily achieving low reflection by optimizing the arc slot of metal plate and the coupling window, the performances of the transformers will directly affect the overall matching characteristics of the OMT.

A. Design of the three multi-section transformers

As is known, the length of the traditional tapered double ridge transition should be long enough to achieve a good reflection coefficient characteristic. It can be explained as follows, the tapered transition in waveguide can be seen as the cascade of infinitely many small steps, and each of them will produce a reflected wave. These reflected waves are always partially cancelled at the input port, so that the total reflected wave can be maintained below a relatively small value across a wide frequency band. However, as the length of the tapered transitions increase, the size of the OMT will become excessively large.

The multi-section transformers can achieve impedance matching more effectively, which can be attributed to the fact that each section's length equals to nearly a quarter center wavelength, corresponding to $0.1875\lambda_{max}$ in the case of 50% fractional working bandwidth. Therefore, the fewer the sections are, the shorter the length will be.

In waveguide devices, since different in-band reflection characteristics can be obtained by assigning different impedance distributions to the multi-section transformers, they have an advantage of design flexibility compared to the traditional tapered one. To design these transformers, the ANSYS HFSS 15 is used, and the model of three transformers are shown in Fig. 3. Each transformer is assigned with the binomial and the Chebyshev impedance distributions, respectively, to verify different in-band responses.

Transformer 1 is a 6-section stepped double ridge waveguide with square waveguide cavity. It achieves an impedance transformation from 87 ohms to 628 ohms, which is calculated by the impedance expressions given in [30]. Transformer 2 is a 5-section double ridge waveguide with a 2-section stepped waveguide cavity, which realizes the impedance matching between 80 ohms and 314 ohms. Transformer 3 is a 4-section E-plane stepped waveguide, which transforms the impedance from 314 ohms to 628 ohms. The length of each section of these transformers is set to be a quarter wavelength of 37.5GHz. The binomial and Chebyshev impedance distributions of each transformer are given in Table 2 and Table 3, respectively.

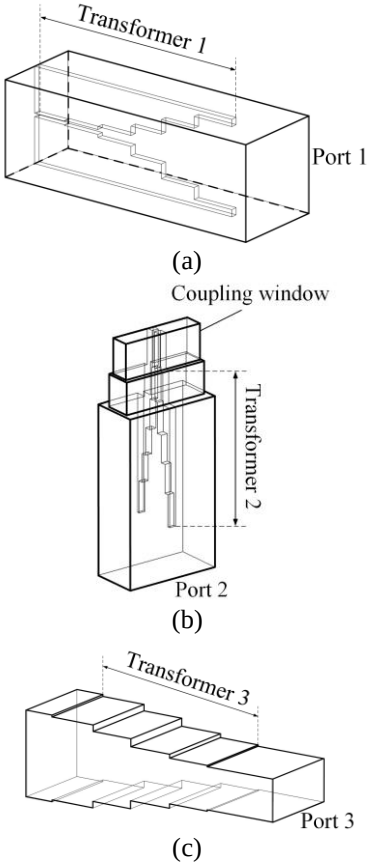

Fig. 3. The schematic of transformers: (a) transformer 1, (b) transformer 2, and (c) transformer 3.

Table 2: The binomial impedance distributions of each transformer

Transformer	1 (ohms)	2 (ohms)	3 (ohms)
1st section	89.7	84.3	328.5
2nd section	108.1	104.8	390.7
3rd section	170.4	161.3	506.5
4th section	310.3	248.3	605.4
5th section	488.9	308.7	
6th section	589.2		

Table 3: The Chebyshev impedance distributions of each transformer

Transformer	1 (ohms)	2 (ohms)	3 (ohms)
1st section	93.0	86.8	330.2
2nd section	118.2	109.9	389.9
3rd section	186.8	161.3	494.5
4th section	326.5	236.9	583.8
5th section	516.0	299.8	
6th section	582.1		

As shown in Fig. 4, the simulation result of the transformer 3 has standard responses of maximally flat and equal ripple characteristics, but the responses of other two transformers both have a little deterioration. This is mainly due to the fact that the double ridge waveguides with different ridge spacing have different cutoff frequency. It will result in the difference between the electrical length of each section and the desired quarter wavelength.

As a result, the binomial impedance distribution has the flattest reflection response, so it can be used to design the ultra-low reflection characteristic in specific frequency band. On the other hand, the Chebyshev impedance distribution has the equal ripple reflection characteristic in band, so it has the widest bandwidth under the limitation of a specified maximum standing wave, making it suitable to design for ultra-wideband applications.

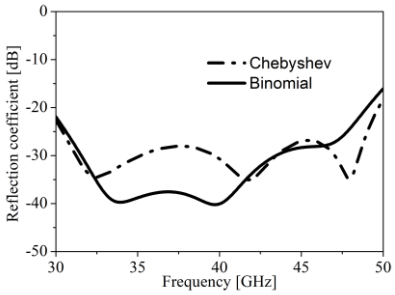

(a)

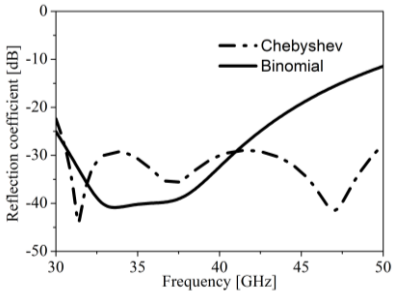

(b)

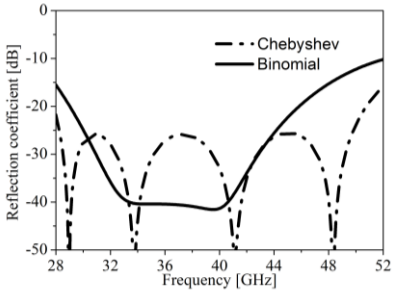

(c)

Fig. 4. The simulated reflection coefficients of each transformer: (a) transformer 1, (b) transformer 2, and (c) transformer 3.

B. Design of the OMT

To work in the 7mm-band, the size of the OMT's three ports refer to the WR-22 standard waveguide, wherein the square one is $5.69\times5.69\text{mm}^2$ and the rectangular one is $5.69\times2.85\text{mm}^2$.

As the performance of the OMT is determined by the 90-degree bend, the coupling window and the three transformers, the first two structures are designed and modeled in Fig. 5. The size of the coupling window is set to be $5\times1.15\times2.1\text{mm}^3$.

Based on the analyses in part A, three transformers with Chebyshev impedance distribution are applied to the 7mm-band OMT design, and their in-band reflection characteristics are optimized by fine-tuning the length of each section. In particular, the 2-section waveguide cavity sizes of the transformer 2 are $5.2\times1.6\times1.9\text{mm}^3$ and $5.69\times2.85\times10.1\text{mm}^3$, respectively. In addition, the absorber is set in the transformer 3 to further reduce the device size, and the parameters of the transformer 3 are listed in Table 4. Other parameters can be obtained in Fig. 6.

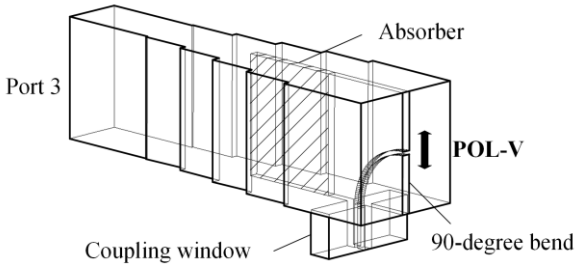

(a)

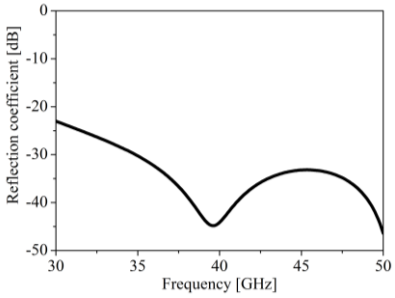

(b)

Fig. 5. Design of the 90-degree bend and the coupling window: (a) simulation model of ANSYS HFSS 15, and (b) reflection coefficient for vertical polarization.

Table 4: The specific parameters and the characteristic impedance of transformer 3

Name	Length (mm)	Width (mm)	Height (mm)
1st step	2.5	5.1	5.69
2nd step	2.5	4.4	
3rd step	2.5	3.6	
4th step	2.5	3	

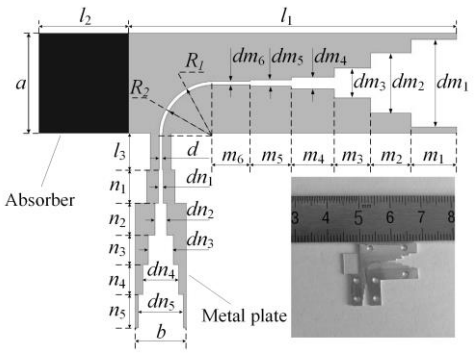

Fig. 6. The sectional view of the metal plate and the absorber. The parameters are (unit: mm): a=5.69, b=2.85, d=0.2, l_1=18.34, l_2=5, l_3=2.1, R_1=3.1, R_2=2.9, m_1=2.56, dm_1=4.99, m_2=2.26, dm_2=3.43, m_3=2.02, dm_3=1.69, m_4=2.4, dm_4=0.66, m_5=2.3, dm_5=0.34, m_6=2, dm_6=0.22, n_1=1.9, dn_1=0.28, n_2=1.8, dn_2=0.65, n_3=1.7, dn_3=1.38, n_4=1.7, dn_4=2, n_5=1.9, dn_5=2.56.

IV. MODELLING AND EXPERIMENTAL RESULTS

The electrical characteristics of the proposed finline OMT are analyzed by using full-wave simulation software ANSYS HFSS 15. To verify the simulated results, a prototype of the OMT has been fabricated, as shown in Fig. 7. In detail, the main body is split into two symmetrical aluminum blocks to manufacture with the help of CNC technique, and the slotted metal plate is fabricated by wire cut processing. Both processes have the tolerance of ±0.02mm. The absorber employs the ITO conductive glass with a surface resistance of 350±100 Ω/cm2. Finally, all parts assemble together with positioning screws and spacing slots.

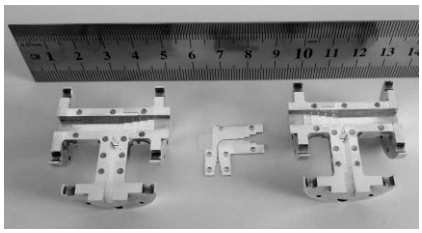

Fig. 7. The picture of the manufactured finline OMT.

The measurement system is composed of a Rohde & Schwarz ZVA 67 vector network analyzer (VNA), two coaxial cable to waveguide converters and a horn antenna used as load. In specific operations, the reflection coefficient and isolation are tested by connecting the OMT's three ports with the VNA and the horn antenna, and the insertion loss is measured with two OMTs arranged in the form of back to back. The simulated and measured results are shown in Fig. 8. Across the working band of 30.2GHz-49.8GHz, the proposed finline OMT possesses the reflection coefficient of less than -20dB, and the insertion loss of less than 1.1dB for both polarizations. Two rectangular ports' isolation is larger than 68dB, and the cross-polarization levels are less than -76dB for both polarizations.

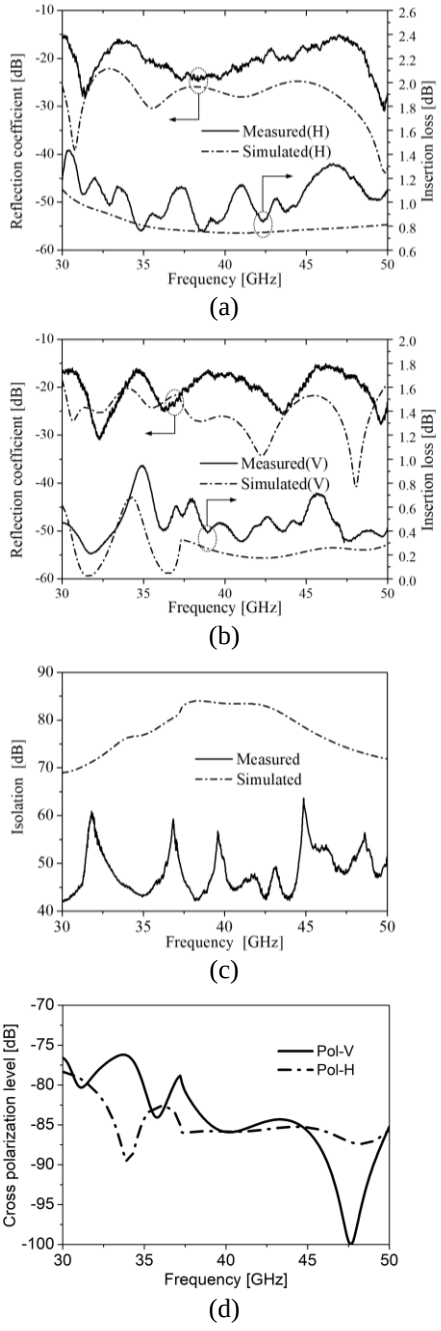

Fig. 8. The simulated and measured results of the proposed OMT: (a) reflection coefficient and insertion loss for horizontal polarization, (b) reflection coefficient and insertion loss for vertical polarization, (c) isolation of port 2 and port 3, and (d) cross-polarization level for both polarizations.

Compared with previous works, the use of multi-section transformers can make the design more compact. Specifically, the length of main arm's and side arm's transition can be reduced to $1.35\lambda_{max}$ and $0.9\lambda_{max}$, respectively.

From the results we can see that the measured ones are slightly worse than the simulated ones. Regardless of the increased reflection and insertion loss introduced by the mounting gaps of the main body, misalignment of waveguide connection interfaces and unstable electrical characteristics of the chosen absorber, the simulated results all have a close trend with the test ones except for the isolation and the reflection coefficient for horizontal polarization. For the former, it is mainly subject to the processing and assembly errors of the OMT. For the latter, the differences are additionally ascribed to the manufacturing and positioning errors of the metal plate.

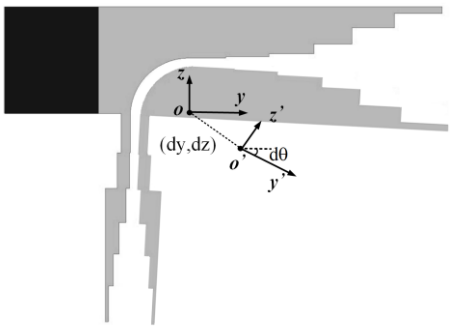

Fig. 9. The schematic of positioning errors.

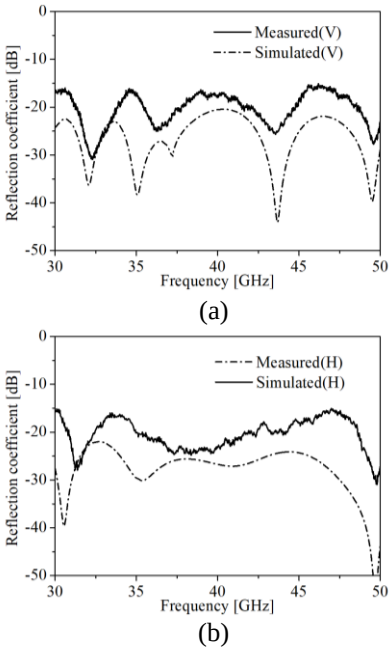

Fig. 10. Reflection coefficient of the measured results of the manufactured OMT and the simulated results of modified model for vertical polarization.

To further understand the effect of the positioning errors on the working performance, the translational error (dy,dz) and rotation error dθ of the metal plate are analyzed, as depicted in Fig. 9.

When (dy,dz)=(-0.01mm,0.04mm) and dθ=0.5deg, the simulated results of the modified model have close resonance frequency points with the measured ones for both polarizations, as shown in Fig. 10. However, due to the influence of the mounting gaps and connection reflection between the OMT and measurement system, the overall reflections will arise.

V. CONCULSION

A compact finline OMT based on multi-section transformer is proposed for operation in 30.2GHz to 49.8 GHz. Under the premise of preserving the in-band working characteristics, the design achieves the size reduction of the OMT. The proposed OMT has been tested and error analyzed. The predicted results have a good agreement with the measured ones.

ACKNOWLEDGMENT

This work was supported by National Basic Research Program of China-973 program 2015CB857100, National Natural Science Foundation of China (No. 61601350, 61401327, 61471278), the Foundation of Chinese Academy of Space Technology (CAST 2015-11).

REFERENCES

[1] R. W. Jackson, "A planar orthomode transducer," *IEEE Microwave and Wireless Components Letters*, vol. 11, (12), pp. 483-485, Dec. 2001.

[2] P. K. Grimes, O. G. King, G. Yassin, and M. E. Jones, "Compact broadband planar orthomode transducer," *Electronics Letters*, vol. 43, (21), pp. 1146-1147, Oct. 2007.

[3] J. Uher, J. Bomemann, and U. Rosenherg, *Waveguide Components for Antenna Feed Systems: Theory and CAD*. Artech House, 1993.

[4] T. J. Reck and G. Chattopadhyay, "A 600 GHz asymmetrical orthogonal mode transducer," *IEEE Microwave and Wireless Components Letters*, vol. 23, (11), pp. 569-571, Sep. 2013.

[5] M. A. Abdelaal, S. I. Shams, and A. A. Kishk, "Asymmetric compact OMT for X-band SAR applications," *IEEE Transactions on Microwave and Techniques*, vol. 66, (4), pp. 1856-1863, Apr. 2018.

[6] D. Dousset, S. Claude, and K. Wu, "A compact high-performance orthomode transducer for the Atacama large millimeter array (ALMA) band 1 (31-45GHz)," *IEEE Access*, 1, pp. 480-487, 2013.

[7] G. Virone, O. A. Peverini, M. Lumia, G. Addamo, and R. Tascone, "Platelet orthomode transducer for Q-band correlation polarimeter clusters," *IEEE Transactions on Microwave Theory and Techniques*,

vol. 62, (7), pp. 1487-1494, June 2014.

[8] J. Y. Han, S. Yoon, T. K. Lee, J. W. Lee, S. Song, and K. Oh, "Turnstile junction ortho-mode transducer for W-band radar seeker," *2016 URSI Asia-Pacific Radio Science Conference (URSI AP-RASC)*, Seoul, South Korea, pp. 1796-1797, Oct. 2016.

[9] J. A. Ruiz-Cruz, J. R. Montejo-Garai, C. A. Leal-Sevillano, and J. M. Rebollar, "Orthomode transducers with folded double-symmetry junctions for broadband and compact antenna feeds," *IEEE Transactions on Antennas and Propagation*, vol. 66, (3), pp. 1160-1168, Jan. 2018.

[10] C. A. Leal-Sevillano, T. J. Reck, G. Chattopadhyay, J. A. Ruiz-Cruz, J. R. Montejo-Garai, and J. M. Rebollar, "Development of a wideband compact orthomode transducer for the 180–270 GHz band," *IEEE Transactions on Terahertz Science and Technology*, vol. 4, (5), pp. 634-636, July 2014.

[11] J. A. Ruiz-Cruz, J. R. Montejo-Garai, C. A. Leal-Sevillano, and J. M. Rebollar, "Development of folded dual-polarization dividers for broadband ortho-mode transducers," *2015 Asia-Pacific Microwave Conference (APMC)*, vol. 2, Nanjing, China, pp. 1-3, Feb. 2016.

[12] S. D. Robertson, "Recent advances in finline circuits," *IRE Transactions on Microwave Theory and Techniques*, 4, (4), pp. 263-267, 1956.

[13] C. E. Groppi, C. Y. Drouet d'Aubigny, A. W. Lichtenberger, and C. M. Lyons, "Broadband finline ortho-mode transducer for the 750-1150 GHz band," *16th International Symposium on Space Terahertz Technology*, Goteborg, Sweden, pp. 513-518, 2005.

[14] S. J. Skinner and G. L. James, "Wide-band ortho-mode transducers," *IEEE Transactions on Microwave and Techniques*, 39, (2), pp. 294-300, Feb. 1991.

[15] G. Chattopadhyay and J. E. Carlstrom, "Finline ortho-mode transducer for millimeter waves," *IEEE Microwave and Guided Wave Letters*, 9, (9), pp. 339-341, 1999.

[16] J. Takeuchi, A. Hirata, H. Takahashi, and N. Kukutsu, "10-Gbit/s bi-directional and 20-Gbit/s uni-directional data transmission over a 120-GHz-band wireless link using a finline ortho-mode transducer," *Microwave Conference Proceedings (APMC)*, Yokohama, Japan, pp. 195-198, 2010.

[17] G. Moorey, R. Bolton, A. Dunning, R. Gough, H. Kanoniuk, and L. Reilly, "A 77-117 GHz cryogenically cooled receiver for radio astronomy," *Proc. of the Workshop on the Applications of Radio Science*, 2006.

[18] M. A. Abdelaal, S. I. Shams, M. A. Moharram, M. Elsaadany, and A. A. Kishk, "Compact full band OMT based on dual-mode double-ridge waveguide," *IEEE Transactions on Microwave and Techniques*, pp. 1-8, Apr. 2018

[19] E. Menargues, S. Capdevila, T. Debogovic, A. Dimitriadis, J. R. Mosig, A. Skrivervik, and E. de Rijk, "Compact orthomode transducer with broadband beamforming capability," *2018 IEEE/MTT-S International Microwave Symposium – IMS*, Philadelphia, USA, Aug. 2018.

[20] G. L. Huang, S. G. Zhou, and T. Yuan, "Design of a compact wideband feed cluster with dual-polarized sum- and difference-patterns implemented via 3-D metal printing," *IEEE Transactions on Industrial Electronics*, vol. 65, (9), pp. 7353-7362, Sep. 2018.

[21] A. Navarrini and Renzo Nesti, "Symmetric reverse-coupling waveguide orthomode transducer for the 3-mm band," *IEEE Transactions on Microwave Theory and Techniques*, vol. 57, (1), Jan. 2009.

[22] A. Dunning, M. Bowen, and Yoon Chung, "Offset quad ridged ortho-mode transducer with a 3.4:1 bandwidth," *2013 Asia-Pacific Microwave Conference Proceedings (APMC)*, Seoul, South Korea, pp. 146-148, Jan. 2014.

[23] A. W. Pollak and M. E. Jones, "A compact quad-ridge orthogonal mode transducer with wide operational bandwidth," *IEEE Antennas and Wireless Propagation Letters*, vol. 17, (3), pp. 422-425, Mar. 2018.

[24] H. Y. Jin, Y. M. Huang, H. L. Jin, and K. Wu, "E-band substrate integrated waveguide orthomode transducer integrated with dual-polarized horn antenna," *IEEE Transactions on Antennas and Propagation*, vol. 66, (5), pp. 2291-2298, May 2018.

[25] A. A. Sakr, W. M. Dyab, and K. Wu, "Theory of polarization-selective coupling and its application to design of planar orthomode transducers," *IEEE Transactions on Antennas and Propagation*, vol. 66, (2), pp. 749-762, Feb. 2018.

[26] B. J. Mohammed, K. S. Bialkowski, and A. M. Abbosh, "Compact stepped slot antenna with unidirectional radiation for animal head imaging system," *2018 Australian Microwave Symposium (AMS)*, Brsibane, Australia, pp. 87-88, Apr. 2018.

[27] M. Knizek, C. Nicholl, C. Popovich, and K. A. Shamaileh, "Quad-band multi-section multi-way power divider and its miniaturization using coupled lines," *2017 IEEE International Symposium on Antennas and Propagation & USNC/URSI National Radio Science Meeting*, San Diego, CA, pp. 2253-2254, Oct. 2017.

[28] R. E. Collin, *Foundations for Microwave Engineerin*g. Cleveland, OH, 1973.

[29] C. Ming, "Novel design method of a multi-section transmission-line transformer using genetic algorithm techniques," *2008 International Conference on Electrical Machines and Systems*, Wuhan, China,

pp. 3793-3796, Feb. 2009.

[30] W. J. R. Hoefer and M. N. Burton, "Closed form expressions for parameters of finned and ridge waveguide," *IEEE Transactions on Microwave and Techniques*, vol. 30, (12), pp. 2190-2194, Dec. 1982.

Yaqing Yu was born in Zhejiang province, China, in October 1990. He received the B.S. degree in Electromagnetic Field and Wireless Technology from Xidian University, Xi'an, China, in 2009. He is currently studying for a doctor's degree in Electromagnetic Field and Microwave Technology from Xidian University. His research interests include wideband antennas, wide beam antennas and antenna feeding structures.

Wen Jiang was born in Shandong province, China, in November 1985. He received the B.S. and Ph.D. degrees from Xidian University, Xi'an, China, in 2008 and 2012, respectively. He is the Vice Director of the National Key Laboratory of Science and Technology on Antennas and Microwaves, Xidian University, where he is currently an Associate Professor. His current research interests include electromagnetic scattering and stealth technology, antenna theory and engineering, and electromagnetic measurement theory and technology.

Shuai Zhang was born in Hubei Province, China, in September 1983. He received the B.S. and Ph.D. degrees from Xidian University, Xi'an, China, in 2007 and 2012, respectively. Now, he teaches at the Electronic Engineering Institute of Xidian University, where he is an Associate Professor. His current research interests include theory and design of antennas and arrays, antenna array radiation calculation and pattern optimization, scattering calculation and electromagnetic stealth design of antennas and arrays and research on radiation and scattering calculation and control methods for large-scale array antennas.

Shuxi Gong was born in Hebei Province, China, in March 1957. He received the B.S. and M.S. degrees from Xidian University, Xi'an, China, in 1982 and 1984, respectively, and the Ph.D. degree from Xi'an Jiaotong University, Xi'an, in 1988. He was the Director of the National Key Laboratory of Science and Technology on Antennas and Microwaves, Xidian University, where he is currently a Full Professor. He has authored or coauthored over 200 refereed journal papers. He has also authored Principles of Generalized Eigenfunction Expansions in Electromagnetic Theory (Xi'an: Xidian Univ. Press, 2010), Prediction and Reduction of Antenna Radar Cross Section (Xi'an: Xidian Univ. Press, 2010), and Antennas for Mobile Communication Systems (Beijing: Electronics Industry Press, 2011). His current research interests include antenna theory and technology, prediction and control of antenna radar cross section (RCS), and RCS calculation of complex targets.

Tong Cheng was born in Hubei, China, in February 1993. He received the B.S. degree in Communication Engineering from Xidian University, Xi'an, China, in 2011. He is currently studying for a doctor's degree in Electromagnetic Field and Microwave Technology from Xidian University. His research interests include substrate integrated waveguide antennas, circularly polarization end-fire antenna and waveguide devices.